International Journal of Environmental Sciences
ISSN: 2229-7359
Vol. 11 No. 19s, 2025
https://theaspd.com/index.php

# Synergistic Co-Delivery Of Berberine Hydrochloride And Amphotericin B Using Mesoporous Silica Nanoparticles: Formulation Strategy And Physicochemical Characterization

**Priyanka Mishra[1], Debmalya Roy[2], Nisha Sharma[1], Kalpana[1], Prakash Chandra Gupta[1], Ram S Bhadauria[3]**

[1]School of Pharmaceutical Sciences, Chhatrapati Shahu Ji Maharaj University, Kanpur - 208024, Uttar Pradesh, India.

[2]Nanoscience and Coating Division, DMSRDE, GT Road, Kanpur, 208013, Uttar Pradesh, India.

[3]Lyka Labs Ltd., Ankleshwar, Bharuch, Gujarat, India.

*Corresponding Author email: nishasharma@csjmu.ac.in

***Abstract***

***Objective:*** *A critical requirement for any nanoparticle intended for drug delivery applications, regardless of the nanocarrier type, is its ability to deliver therapeutic agents precisely to target sites within the body, thereby enhancing effectiveness and minimizing adverse effects. Consequently, when designing a nanocarrier, it is essential to account for its biological interactions and behaviour upon administration. This study reports the synthesis of mesoporous silica nanoparticles (MSNPs) co-encapsulating Berberine hydrochloride and Amphotericin B, synthesized via a sol-gel method.*

***Method:*** *The study provides a comprehensive evaluation of the synthesis and characterization of mesoporous silica nanoparticles encapsulating Berberine hydrochloride and Amphotericin B. Various parameters, including particle size, polydispersity index, surface morphology, drug loading capacity, zeta potential, entrapment efficiency, and release behaviour, were systematically analysed.*

***Results:*** *The blank mesoporous silica nanoparticles had an average diameter of 210 ± 3.8 nm, with a polydispersity index (PDI) of 0.304 ± 0.065, and carried a zeta potential of −21.2 ± 1.3 mV. After co-loading Berberine hydrochloride and Amphotericin B (forming the BBR-AMB-MSNPs), the optimized formulation increased slightly in size to 260 ± 3.5 nm, with a PDI of 0.353 ± 0.012 and a zeta potential similarly around −27 ± 4.5 mV. It achieved high encapsulation efficiencies BBR and AMB of range 68.20±3.4 % to 75.34±2.3 and 62.23±1.8 % to 70.55±2.4, respectively. Spectroscopic and microscopic examinations verified that both drugs were successfully entrapped within the silica matrix. Meanwhile, in vitro drug-release assays revealed a controlled release pattern for both active agents.*

***Conclusions:*** *The formulation strategy led to a robust, well-characterized mesoporous silica nanoparticle capable of effectively delivering both Berberine HCl and Amphotericin B. The optimized BBR-AMB-MSNP platform exhibits promising physicochemical properties appropriate size, uniformity and high entrapment efficiency alongside desirable in vitro release behaviour.*

***Keywords:*** *Mesoporous silica nanoparticles, Polydispersity index, Berberine HCl, Amphotericin B, Physicochemical properties, Entrapment efficiency*

## INTRODUCTION:

The swift advancement of nanotechnology has revealed the significant potential of nanomaterials in the biomedical sector, attributed to their superior physicochemical characteristics. Range of nano carriers has been extensively investigated and produced for cargo transportation, illness diagnostics, and therapeutic applications [1]. In comparison to macroscale counterparts, nano formulations consistently exhibit distinct advantages, such as enhanced bioavailability, diminished harmful effects, and increased selectivity inside living organisms [2]. Nano formulations generally comprise two primary categories: organic and inorganic nano formulations [3-4]. Inorganic nanoparticle-based formulations, are biocompatible and safe than their organic counterparts, exhibit higher stability and drug delivery efficiency. Significantly, the distinctive characteristics of inorganic nanoparticles, including optical, ultrasonic, magnetic, and catalytic properties, have led to the development of innovative nanoparticle-based therapies [5-6]. Promisingly, inorganic nanoparticles are progressively advancing to the clinical stage, with approximately 25 inorganic nanomedicines sanctioned for clinical application. MSNP are significant interest to researchers globally among other inorganic nanoparticle-based formulations due to their remarkable versatility in structural and property adjustment [7-8]. MSNP exhibit a wide array of modifiable specific surface areas, pore sizes,

customizable particle size, morphologies, and facile surface functionalization. MSNP can serve as substrate materials for the incorporation of nanomaterials such as carbon dots, gold nanoparticles, and iron oxide nanoparticles, leading to inorganic nanocomposites with varied characteristics suitable for numerous biomedical applications [9]. We may manipulate the synthesis circumstances to accurately adjust the topology and achieve superior internal and surface architecture of MSNP, hence attaining the desired performance [10-13]. The commonly utilized food additive comprises amorphous silica nanoparticles with a diameter of 100 nm [14].

Berberine hydrochloride ($C_{20}H_{18}ClNO_4$) is a quaternary ammonium isoquinoline alkaloid, crystallizes into needle-shaped yellow crystals. Due to its low solubility in water, BBR experiences rapid metabolism, self-aggregation, localized dissolution, elimination, and clearance [15]. This indicates reduced clinical efficacy, less cellular bioavailability, and lower intestine absorption activity. Adverse consequences of high BBR dosages that may negate its therapeutic benefits include anorexia, gastrointestinal discomfort, diarrhoea, and constipation. To enhance medicine delivery systems, it is essential to produce MSNP infused with BBR. The creation of MSNP infused with BBR is crucial for the progression of drug delivery systems [16].

In comparison to certain existing drug delivery carriers, the active constituents of herbal medicine utilized as nanocarriers may exhibit enhanced biocompatibility, reduced toxicity and adverse reactions, and possess pharmacological activity that can synergistically interact with the encapsulated drug, yielding a drug-assisted combined effect [17-19]. Berberine and amphotericin B naturally self-assemble to create mesoporous silica nanoparticles, which markedly improve their activity [20]. This study was performed to design Mesoporous Silica Nanoparticles for the co delivery of Berberine hydrochloride and Amphotericin B and Physicochemical Characterization.

## 3. MATERIALS AND METHODS

### 3.1 Materials

The drug amphotericin B was a generous gift from Sumar Biotech LLP, Mehsana, Gujrat. Berberine hydrochloride was purchased from TCI Mumbai, India. HCL (37% concentration), DMSO, tetraethyl orthosilicate (TEOS), hexadecyl trimethyl ammonium bromide (CTAB), sodium dihydrogen phosphate, potassium chloride, ammonium chloride, disodium hydrogen phosphate, and acetic acid were all of analytical grades.

### 3.2 Surface Functionalization of MSNP

MSNPs were used for the functionalization. Briefly, a of MSNP were added to polyethene glycol 200 and dispersed in deionized water magnetic stirrer, followed by keeping the dispersion for 30 min in a bath sonicator. The resulting mixture was then subjected to a high-speed centrifuge at 12000 rpm for 30 min. After centrifugation, the supernatant was discarded and the sediment was collected in a petri plate and dried in an oven at 80℃ for overnight. After drying, the sample was transferred to a container and stored and further use in the formulation development [21-24].

### 3.3 Optimization and formulation development of BBR-AMB Loaded MSNPs

Formulation optimization was carried out with varying the concentration of drug ratio, sonication time, stirring speed. For the best optimized formulation known quantity of dried MSNP were taken in a beaker and deionized water was added. The mixture was sonicated for 30 min under bath sonication. After sonication, BBR and AMB were added to the MSNP mixture and kept aside for stirring for 6 hours. Particle size was analysed using Malvern particle size analyser.

## 4. Characterization of optimized formulation

The functionalized mesoporous silica nanoparticles and their formulations were meticulously examined utilizing analytical methods to assess particle size, dispersion, morphology. Surface morphology and particle size were examined with a SEM and particle size analyser. Particle size analysis was conducted using a Nano Zetasizer (ZS) from Malvern Instruments (Malvern, UK), which elucidated the influence of numerous parameters on the attributes of the formulations. All measurements were conduct in triplicate, and mean values were utilized to compute polydispersity index (PDI) and particle size. Entrapment efficiency and release behaviour were determined using a standard calibration curve.

### 4.1 Size, polydispersity index and zeta potential

The formulated samples were loaded into cuvettes and assessed for their particle size polydispersity index, and zeta potential at room temperature using a Malvern particle size analyser (Model EN1690, Malvern Instruments, UK) [25].

**4.2 Fourier Transform Infra-Red Spectroscopy (FTIR)**

A Fourier transform infrared (FTIR) analysis was performed on Berberine HCl, Amphotericin B, mesoporous silica nanoparticles, and the optimized drug-loaded formulation using the KBr pellet technique on a FT-IR/FIR instrument. The pellets were prepared by blending each sample with potassium bromide in a 1:10 proportion. These pellets were then placed in the sample holder and scanned over the spectral range of 4000 to 400 $cm^{-1}$ [26].

**4.3 AFM Analysis**

Atomic force microscopy (AFM) enables three-dimensional analysis of a samples, ranging from conductive and insulating materials to inorganic, organic, and biological specimens, and can function in both air and liquid media. The surface roughness of the optimized formulation was assessed by AFM instrument. For analysis, a thin film was created by placing a drop of the dispersion onto a glass slide and spreading it with a spin coater [27].

**4.4 Scanning Electron Microscopy (SEM)**

The optimized formulation was analysed utilizing FESEM. This sophisticated imaging method yielded intricate micrographs, facilitating a precise examination of the nanoparticles' shape and structural attributes. These particles exhibited a homogeneous spherical morphology, indicative of their organized and consistent structural characteristics. The MIRA3 FEG-SEM facilitated accurate size measurements and provided significant insights into the spherical structure of the synthesized MSNP [28].

**4.5 Entrapment Efficiency**

The encapsulation performance of several formulations of MSNP containing BBR and AMB were evaluated by measuring the quantity of unencapsulated medication in the surrounding medium. A 3 ml aliquot of sample was placed in a centrifuge tube and centrifuged at 21,000 rpm for 30 minutes. Subsequent to centrifugation, the supernatant was meticulously filtered utilizing Whatman filter paper. The supernatant was analysed with a UV–visible spectrophotometer (Model 1700, Shimadzu, Japan) at 345 nm (BBR) and 405 nm (AMB). The percentage of medication contained within the nanoparticles was determined using a conventional formula as indicated by the following equation [29].

$$\textbf{Encapsulation efficiency (\%)} = \frac{\textbf{Amount of drug use—Amount of untrapped drug}}{\textbf{Amount of drug use in formulation}} \times 100$$

**4.6 In-Vitro Drug Release:**

The drug release profile of the prepared formulations examined under physiological conditions at pH 7.4. In this procedure, 2 mL of the formulation was placed inside a dialysis membrane and immersed in 50 mL of Phosphate Buffer Saline (PBS) at 37°C within a shaking water bath. Samples of 1 mL were withdrawn from the PBS medium at predetermined intervals between 15 minutes and 48 hours for analysis using a UV-visible spectrophotometer. To preserve the system's volume, an equal amount of fresh PBS was replenished after each sampling [30-31].

**5. Results and Discussion.**

**5.1 Determination of size and PDI:**

The particle sizes of various formulations containing BBR-AMB within MSNP were evaluated. Among these, the optimized formulation demonstrated a particle size of 260 ± 3.5 nm and a polydispersity index (PDI) of 0.353 ± 0.012. Across all tested silica nanoparticles, the range of blank silica with size from 121.88 ± 2.5 nm to 271.45 ± 8.22 nm, with PDI values between 0.244 ± 0.016 and 0.362 ± 0.007. Particle size plays a significant role in cellular uptake and the stability of colloidal systems, with the PDI serving as a measure of size uniformity. Generally, PDI values above 0.7 indicate a wide particle size distribution, which is undesirable. Nanoparticles with PDI values below 0.4 are considered to have a more uniform size distribution and reduced aggregation tendencies [32].

**Table.1:** Results of size, PDI, zeta potential, entrapment efficiency

| Sample code | Particle size (nm) | Poly dispersity index (PDI) | Zeta potential (mV) | Entrapment Efficiency (%) |
|---|---|---|---|---|
| **MSNP** | 210±3.8 | 0.304±0.065 | -21.2±1.3 | ------ |
| **BBR-AMB MSNP** | 260±3.5 | 0.353±0.012 | -27.0±4.5 | 72.44±2.3 BBR 61.23±1.8 AMB |

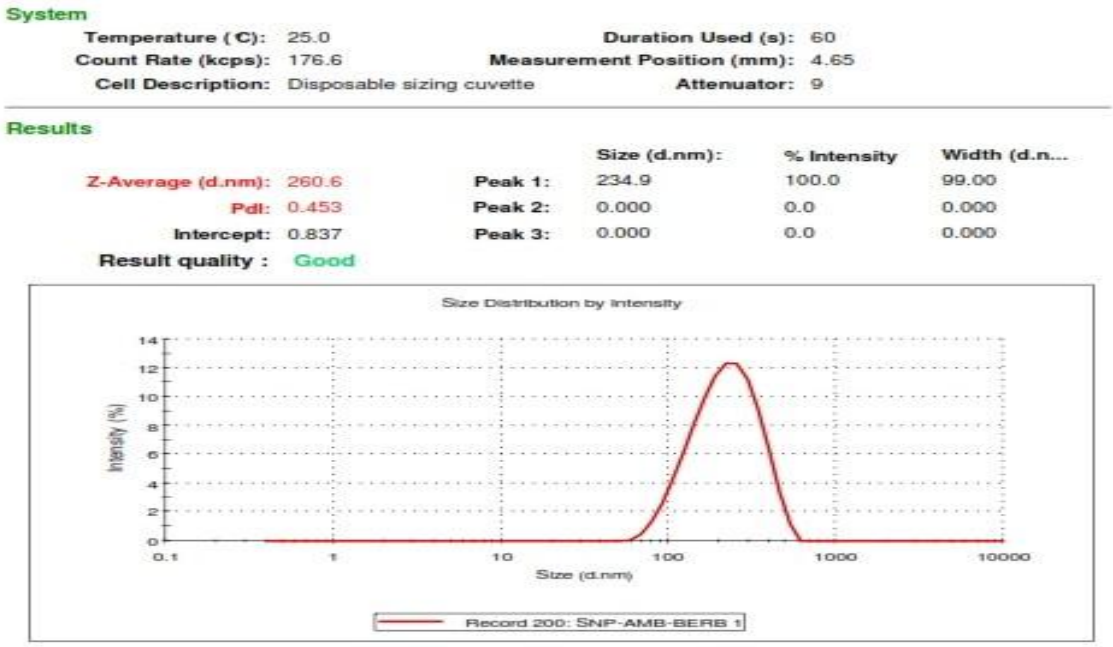


**Fig. 1. Particle size distribution and PDI of BBR-AMB loaded MSNP**

**5.2 Zeta Potential Determination**

The zeta potential of various BBR-AMB-loaded silica nanoparticle formulations was assessed to evaluate colloidal stability. Among them, the optimized formulation exhibited a zeta potential value of −27 ± 4.5 mV. It serves as a crucial parameter for determining the stability of nanoparticulate systems, as it reflects the surface charge and the extent of electrostatic repulsion between particles. The magnitude of zeta potential is influenced by factors such as particle dispersion, agglomeration, and the tendency to flocculate. Formulations incorporating anionic surfactants tend to show reduced aggregation due to increased repulsive forces between vesicles. MSNP are considered stable when their zeta potential lies within the range of +30 mV to −30 mV. In our study, the optimized formulation designated as Formulation F6 exhibited a narrow size distribution, good colloidal stability, and no visible signs of particle clumping, supporting its suitability potential for drug delivery applications [33].

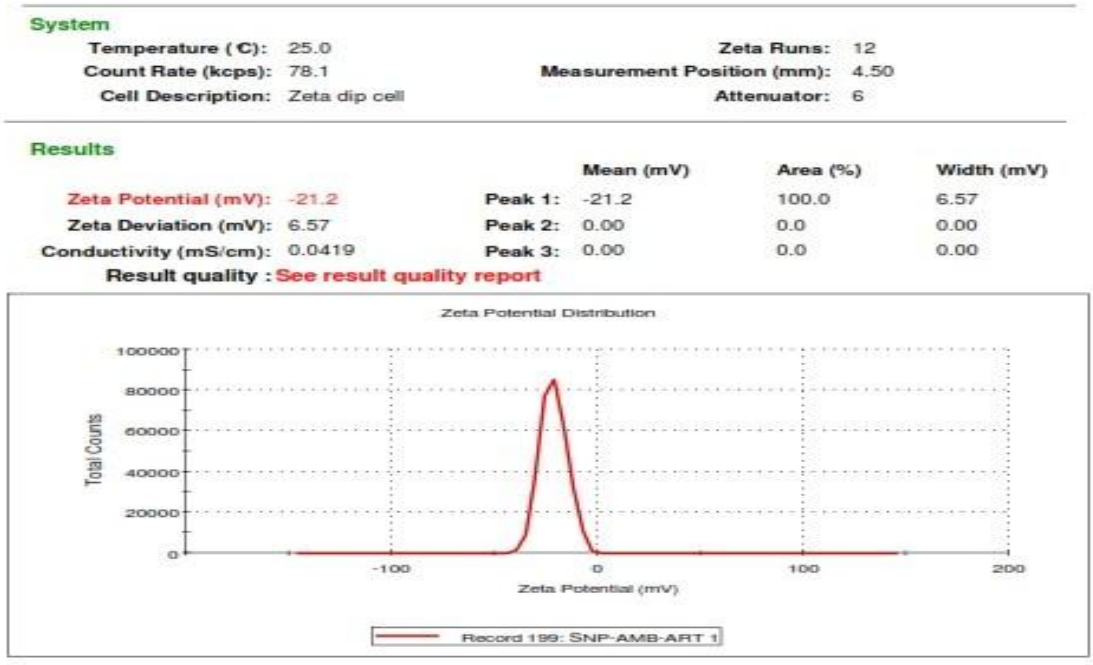


**Fig. 2. Zeta potential of Blank MSNP**

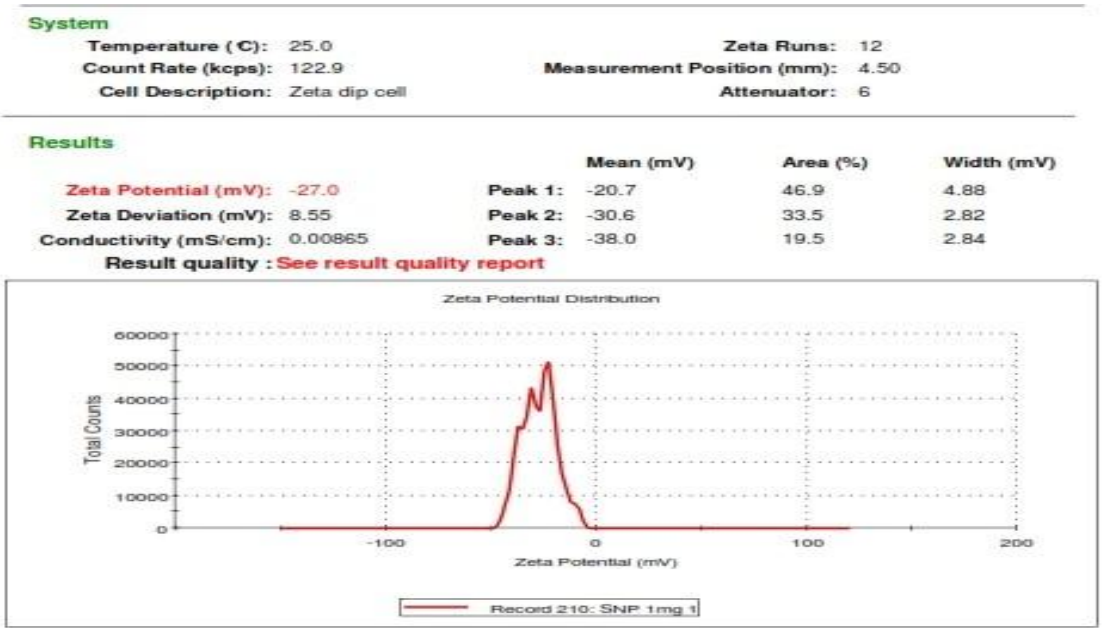


**Fig. 3. Zeta potential of BBR-AMB loaded MSNP**

### 5.3 FTIR study

FTIR spectroscopy was utilized to analyze pure berberine HCl, amphotericin B, mesoporous silica nanoparticles (MSNPs), and their physical combination to identify functional groups and potential interactions. The spectra revealed all characteristic peaks corresponding to berberine HCl and amphotericin B, both individually and in the physical mixture, without any new peaks emerging. This suggests that there were no chemical interactions between two drugs, indicating their compatibility [34].

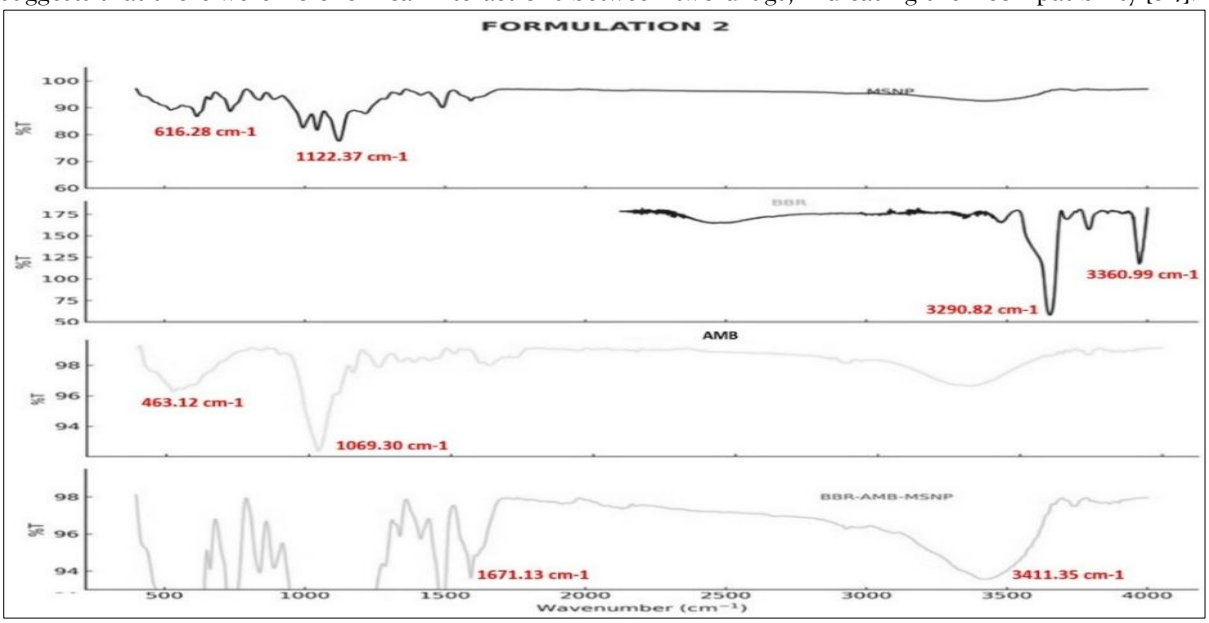


**Fig. 4. (1) FTIR Spectra of MSNP (2) FTIR Spectra of Berberine (3) FTIR Spectra of Amphotericin B (4) FTIR Spectra of physical mixture of BBR-AMB-MSNP**

### 5.4 Morphological Characterization:

Scanning Electron Microscopy (SEM) demonstrated that the refined preparation method successfully generated BBR-AMB loaded nanoparticles utilizing Tween 80 as the surfactant (Figure 5). The examination of the SEM images revealed the morphological features of the MSNP [35]. The surface morphology of the mesoporous silica nanoparticle solution on glass surfaces was examined using AFM analysis. The 3D AFM pictures from Figure 6 can be understood as topographic maps of the material.

International Journal of Environmental Sciences
ISSN: 2229-7359
Vol. 11 No. 19s, 2025
https://theaspd.com/index.php

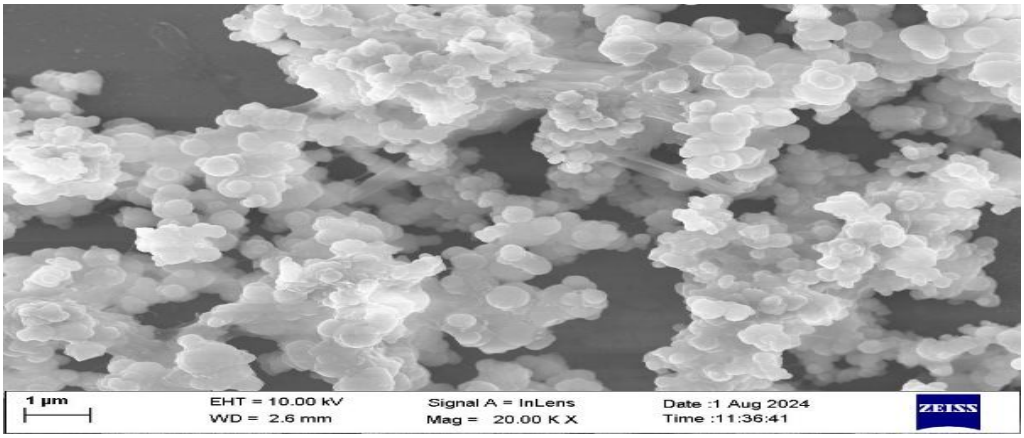


**Fig. 5. SEM analysis of BBR-AMB loaded MSNP**

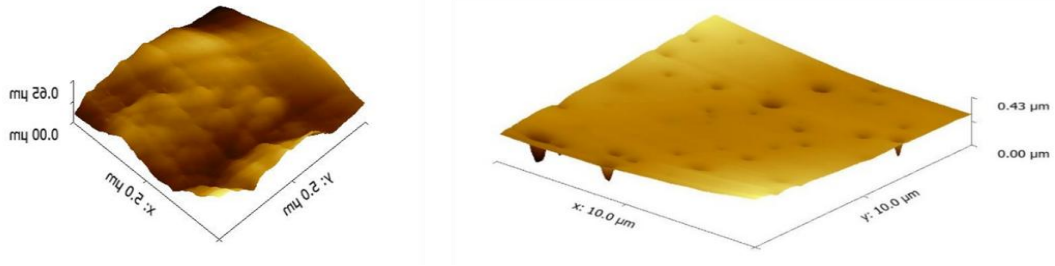


**Fig. 6. Three-dimensional (3D) AFM images of BBR-AMB loaded MSNP**

**5.5 Encapsulation Efficiency:**

The encapsulation efficiencies of berberine HCl and Amphotericin B ranges from 68.20±3.4 % to 75.34±2.3 and 62.23±1.8 % to 70.55±2.4, respectively. Such integration can create transient pores, enhance membrane fluidity and facilitate drug leakage. Moreover, higher concentrations of surfactant promote the formation of numerous vesicles, expanding the content of the hydrophobic bilayer region available to adjust the lipophilic drugs thereby boosting overall encapsulation Specifically for berberine HCl, its high entrapment likely benefits from this increased hydrophobic bilayer capacity [36].

**5.6 In vitro release study.**

In vitro release profile was conducted to evaluate how berberine HCl and Amphotericin B were released from the optimized nanoparticle system under physiological conditions (pH 7.4). Utilizing a dialysis bag (DM-110) method, the in vitro dissolution was monitored over a 48-hour period in both acidic and alkaline media. The release pattern of BBR and AMB occurred in two distinct phases. Initially, a controlled release took place over 6 hours, characterized by a quick release accounting for approximately 25% of the encapsulated BBR and AMB. This was followed by a control release phase over 48 hours, reaching cumulative release levels of around 69–78 % for BBR and 60–70% for AMB. These results indicated the prolonged retention of the drugs within the MSNPs at pH 7.4. These findings indicate that the formulation achieves controlled release for both drugs, which may enhance their therapeutic effectiveness.

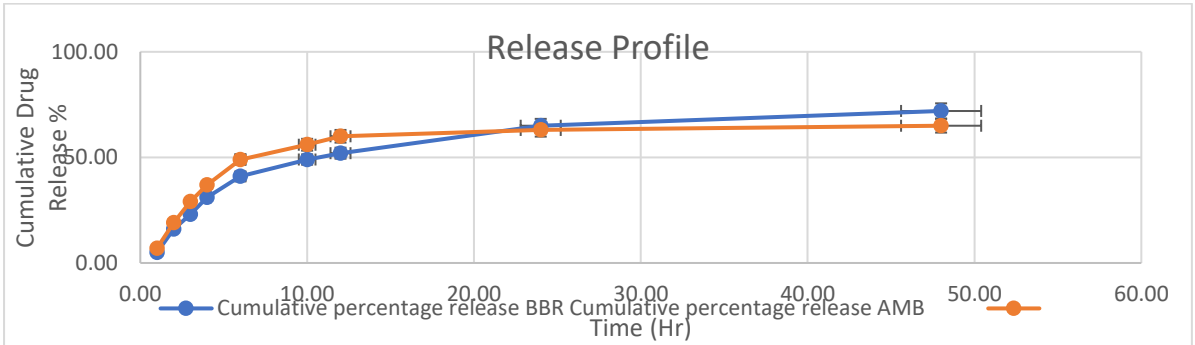


**Fig.7: Measured cumulative drug release vs. time profile at pH 7.4**

## CONCLUSIONS

This paper details the co-formulation and refinement of mesoporous silica nanoparticles (MSNs) designed to deliver both Berberine HCl and Amphotericin B. Optimized dual-drug MSNPs achieved a mean particle diameter of $260 \pm 3.5$ nm, PDI of $0.353 \pm 0.012$ and zeta potential similarly around $-27 \pm 4.5$ mV, with high encapsulation efficiencies of for Berberine HCl and Amphotericin B. Best formulation demonstrated drug release, with $75.08 \pm 0.71\%$ for Berberine HCl and $66.07 \pm 3.91\%$ for Amphotericin B which released over 48 hours an indication of the formulation's potential for enhanced therapeutic outcomes. Initial characterization confirmed favourable nanoparticle properties, including a narrow size distribution, low PDI and consistent zeta potential, supporting their structural stability and suitability for administration. The high drug encapsulation, controlled release, and appropriate physicochemical attributes suggest that these MSNs are a promising drug delivery.

**REFERENCES:**

[1] Ickenstein, L. M., and Garidel, P., 2019, "Lipid-Based Nanoparticle Formulations for Small Molecules and RNA Drugs," Expert Opinion on Drug Delivery, 16(11), pp. 1205–1226. https://doi.org/10.1080/17425247.2019.1669558.
[2] Manzano, M., and Vallet-Regí, M., 2019, "Mesoporous Silica Nanoparticles for Drug Delivery," Adv Funct Materials, 30(2). https://doi.org/10.1002/adfm.201902634.
[3] Parra-Nieto, J., del Cid, M. A. G., de Cárcer, I. A., and Baeza, A., 2020, "Inorganic Porous Nanoparticles for Drug Delivery in Antitumoral Therapy," Biotechnology Journal, 16(2). https://doi.org/10.1002/biot.202000150.
[4] Chen, L., Hong, W., Ren, W., Xu, T., Qian, Z., and He, Z., 2021, "Recent Progress in Targeted Delivery Vectors Based on Biomimetic Nanoparticles," Sig Transduct Target Ther, 6(1). https://doi.org/10.1038/s41392-021-00631-2.
[5] Farzin, A., Etesami, S. A., Quint, J., Memic, A., and Tamayol, A., 2020, "Magnetic Nanoparticles in Cancer Therapy and Diagnosis," Adv Healthcare Materials, 9(9). https://doi.org/10.1002/adhm.201901058.
[6] Xu, H., Li, S., and Liu, Y.-S., 2022, "Nanoparticles in the Diagnosis and Treatment of Vascular Aging and Related Diseases," Sig Transduct Target Ther, 7(1). https://doi.org/10.1038/s41392-022-01082-z.
[7] Germain, M., Caputo, F., Metcalfe, S., Tosi, G., Spring, K., Åslund, A. K. O., Pottier, A., Schiffelers, R., Ceccaldi, A., and Schmid, R., 2020, "Delivering the Power of Nanomedicine to Patients Today," Journal of Controlled Release, 326, pp. 164–171. https://doi.org/10.1016/j.jconrel.2020.07.007.
[8] Mitchell, M. J., Billingsley, M. M., Haley, R. M., Wechsler, M. E., Peppas, N. A., and Langer, R., 2020, "Engineering Precision Nanoparticles for Drug Delivery," Nat Rev Drug Discov, 20(2), pp. 101–124. https://doi.org/10.1038/s41573-020-0090-8.
[9] Wang, Y., Meng, H.-M., and Li, Z., 2021, "Near-Infrared Inorganic Nanomaterial-Based Nanosystems for Photothermal Therapy," Nanoscale, 13(19), pp. 8751–8772. https://doi.org/10.1039/d1nr00323b.
[10] Younis, M. R., He, G., Qu, J., Lin, J., Huang, P., and Xia, X., 2021, "Inorganic Nanomaterials with Intrinsic Singlet Oxygen Generation for Photodynamic Therapy," Advanced Science, 8(21). https://doi.org/10.1002/advs.202102587.
[11] Sun, L., Wang, P., Zhang, J., Sun, Y., Sun, S., Xu, M., Zhang, L., Wang, S., Liang, X., and Cui, L., 2021, "Design and Application of Inorganic Nanoparticles for Sonodynamic Cancer Therapy," Biomater. Sci., 9(6), pp. 1945–1960. https://doi.org/10.1039/d0bm01875a.
[12] Hao, Y.-N., Zhang, W.-X., Gao, Y.-R., Wei, Y.-N., Shu, Y., and Wang, J.-H., 2021, "State-of-the-Art Advances of Copper-Based Nanostructures in the Enhancement of Chemodynamic Therapy," J. Mater. Chem. B, 9(2), pp. 250–266. https://doi.org/10.1039/d0tb02360d.
[13] Huang, Y., Wu, S., Zhang, L., Deng, Q., Ren, J., and Qu, X., 2022, "A Metabolic Multistage Glutathione Depletion Used for Tumor-Specific Chemodynamic Therapy," ACS Nano, 16(3), pp. 4228–4238. https://doi.org/10.1021/acsnano.1c10231.
[14] Xu, B., Wang, H., Wang, W., Gao, L., Li, S., Pan, X., Wang, H., Yang, H., Meng, X., Wu, Q., Zheng, L., Chen, S., Shi, X., Fan, K., Yan, X., and Liu, H., 2019, "A Single-Atom Nanozyme for Wound Disinfection Applications," Angew Chem Int Ed, 58(15), pp. 4911–4916. https://doi.org/10.1002/anie.201813994.
[15] Huang, H., Feng, W., Chen, Y., and Shi, J., 2020, "Inorganic Nanoparticles in Clinical Trials and Translations," Nano Today, 35, p. 100972. https://doi.org/10.1016/j.nantod.2020.100972.
[16] Nguyen, T. L., Choi, Y., and Kim, J., 2018, "Mesoporous Silica as a Versatile Platform for Cancer Immunotherapy," Advanced Materials, 31(34). https://doi.org/10.1002/adma.201803953.
[17] Janjua, T. I., Cao, Y., Yu, C., and Popat, A., 2021, "Clinical Translation of Silica Nanoparticles," Nat Rev Mater, 6(12), pp. 1072–1074. https://doi.org/10.1038/s41578-021-00385-x.
[18] Mishra, G., Awasthi, R., Singh, A. K., Singh, S., Mishra, S. K., Singh, S. K., and Nandi, M. K., 2022, "RETRACTED: Intranasally Co-Administered Berberine and Curcumin Loaded in Transfersomal Vesicles Improved Inhibition of Amyloid Formation and BACE-1," ACS Omega, 7(47), pp. 43290–43305. https://doi.org/10.1021/acsomega.2c06215.
[19] Dahiya, M., Awasthi, R., Yadav, J. P., Sharma, S., Dua, K., and Dureja, H., 2023, "Chitosan Based Sorafenib Tosylate Loaded Magnetic Nanoparticles: Formulation and in-Vitro Characterization," International Journal of Biological Macromolecules, 242, p. 124919. https://doi.org/10.1016/j.ijbiomac.2023.124919.
[20] Kaur, K., Kumar, P., and Kush, P., 2020, "Amphotericin B Loaded Ethyl Cellulose Nanoparticles with Magnified Oral Bioavailability for Safe and Effective Treatment of Fungal Infection," Biomedicine & Pharmacotherapy, 128, p. 110297. https://doi.org/10.1016/j.biopha.2020.110297.
[21] Singh, A. K., Singh, S. S., Rathore, A. S., Singh, S. P., Mishra, G., Awasthi, R., Mishra, S. K., Gautam, V., and Singh, S. K., 2021, "Lipid-Coated MCM-41 Mesoporous Silica Nanoparticles Loaded with Berberine Improved Inhibition of Acetylcholine Esterase and Amyloid Formation," ACS Biomater. Sci. Eng., 7(8), pp. 3737–3753. https://doi.org/10.1021/acsbiomaterials.1c00514.

[22] Mahdi, A. E., Ali, N. S., Majdi, H. Sh., Albayati, T. M., Abdulrahman, M. A., Jasim, D. J., Kalash, K. R., and Salih, I. K., 2023, "Effective Adsorption of 2-Nitroaniline from Wastewater Applying Mesoporous Material MCM-48: Equilibrium, Isotherm, and Mechanism Investigation," Desalination and Water Treatment, 300, pp. 120–129. https://doi.org/10.5004/dwt.2023.29741.
[23] Albayati, T. M., Salih, I. K., and Alazzawi, H. F., 2019, "Synthesis and Characterization of a Modified Surface of SBA-15 Mesoporous Silica for a Chloramphenicol Drug Delivery System," Heliyon, 5(10), p. e02539. https://doi.org/10.1016/j.heliyon.2019.e02539.
[24] Ali, N. S., Albayati, T. M., and Salih, I. K., 2024, "Studying the Kinetics and Removal Mechanism of the Methylene Blue Dye in a Continuous Adsorption Process Using Prepared Mesoporous Materials," Water Practice & Technology, 19(7), pp. 2799–2815. https://doi.org/10.2166/wpt.2024.162.
[25] Kazemzadeh, P., Sayadi, K., Toolabi, A., Sayadi, J., Zeraati, M., Chauhan, N. P. S., and Sargazi, G., 2022, "Structure-Property Relationship for Different Mesoporous Silica Nanoparticles and Its Drug Delivery Applications: A Review," Front. Chem., 10. https://doi.org/10.3389/fchem.2022.823785.
[26] Sahibzada, M. U. K., Sadiq, A., Faidah, H. S., Khurram, M., Amin, M. U., Haseeb, A., and Kakar, M., 2018, "Berberine Nanoparticles with Enhanced in Vitro Bioavailability: Characterization and Antimicrobial Activity," DDDT, Volume 12, pp. 303–312. https://doi.org/10.2147/dddt.s156123
[27] Jiang, X., Tang, X., Tang, L., Zhang, B., and Mao, H., 2019, "Synthesis and Formation Mechanism of Amorphous Silica Particles via Sol–Gel Process with Tetraethylorthosilicate," Ceramics International, 45(6), pp. 7673–7680. https://doi.org/10.1016/j.ceramint.2019.01.067.
[28] Dhavale, R. P., Nadaf, S. J., and Bhatia, M. S., 2021, "Quantitative Structure Property Relationship Assisted Development of Fluocinolone Acetonide Loaded Transfersomes for Targeted Delivery," Journal of Drug Delivery Science and Technology, 65, p. 102758. https://doi.org/10.1016/j.jddst.2021.102758.
[29] Solanki, R., Patel, K., and Patel, S., 2021, "Bovine Serum Albumin Nanoparticles for the Efficient Delivery of Berberine: Preparation, Characterization and In Vitro Biological Studies," Colloids and Surfaces A: Physicochemical and Engineering Aspects, 608, p. 125501. https://doi.org/10.1016/j.colsurfa.2020.125501.
[30] Kuang, G., Zhang, Q., He, S., and Liu, Y., 2020, "Curcumin-Loaded PEGylated Mesoporous Silica Nanoparticles for Effective Photodynamic Therapy," RSC Adv., 10(41), pp. 24624–24630. https://doi.org/10.1039/d0ra04778c.
[31] Usgodaarachchi, L., Thambiliyagodage, C., Wijesekera, R., and Bakker, M. G., 2021, "Synthesis of Mesoporous Silica Nanoparticles Derived from Rice Husk and Surface-Controlled Amine Functionalization for Efficient Adsorption of Methylene Blue from Aqueous Solution," Current Research in Green and Sustainable Chemistry, 4, p. 100116. https://doi.org/10.1016/j.crgsc.2021.100116.
[32] Wise, A. J., Sefy, J. S., Barbu, E., O'Malley, A. J., van der Merwe, S. M., and Cox, P. A., 2020, "Zero-Order and Prolonged Release of Atenolol from Microporous FAU and BEA Zeolites, and Mesoporous MCM-41: Experimental and Theoretical Investigations," Journal of Controlled Release, 327, pp. 140–149. https://doi.org/10.1016/j.jconrel.2020.07.027.
[33] Zhang, F., Zhang, M., Zheng, X., Tao, S., Zhang, Z., Sun, M., Song, Y., Zhang, J., Shao, D., He, K., Li, J., Yang, B., and Chen, L., 2018, "Berberine-Based Carbon Dots for Selective and Safe Cancer Theranostics," RSC Adv., 8(3), pp. 1168–1173. https://doi.org/10.1039/c7ra12069a.
[34] Wang, M., Xia, H., Yang, X., Zhang, Q., Li, Y., Wang, Y., Xia, Y., and Xie, Z., 2023, "Berberine Hydrochloride-Loaded Liposomes Gel: Preparation, Characterization and Antioxidant Activity," Ind. J. Pharm. Edu. Res, 57(1), pp. 74–82. https://doi.org/10.5530/001954642087.
[35] Raval, N., Maheshwari, R., Kalyane, D., Youngren-Ortiz, S. R., Chougule, M. B., and Tekade, R. K., 2019, "Importance of Physicochemical Characterization of Nanoparticles in Pharmaceutical Product Development," Basic Fundamentals of Drug Delivery, pp. 369–400. https://doi.org/10.1016/b978-0-12-817909-3.00010-8.
[36] Zhu, H., Chen, X., Ahmed, M., Wang, Y., Liu, Q., Uppoor, R. S., Kuemmel, C., and Mehta, M., 2019, "A Proposal of Conducting Bioequivalence Trials with Gastric pH Modulators for Two Oral Formulations Demonstrating Different Dissolution Profiles at Elevated pH," Clinical Translational Sci, 12(6), pp. 564–572. https://doi.org/10.1111/cts.12658.
[37] Tahan, M., Zeraatkar, S., Neshani, A., Marouzi, P., Behmadi, M., Alavi, S. J., Hashemi Shahri, S. H., and Hosseini Bafghi, M., 2023, "Antibacterial Potential of Biosynthesized Silver Nanoparticles Using Berberine Extract Against Multidrug-Resistant Acinetobacter Baumannii and Pseudomonas Aeruginosa," Indian J Microbiol, 64(1), pp. 125–132. https://doi.org/10.1007/s12088-023-01136-y.